Radiation Pattern Correction of Faulty Planar Phased Array using Genetic Algorithm

Raja Aasim B. Saleem[1], Arslan A. Shah[1], Hina Munsif[1], Ali I. Najam[2], Shahid Khattak[1] and Irfanullah[1]

[1]Department of Electrical and Computer Engineering, COMSATS University Islamabad, Abbottabad Campus, P.O. Box 22060, Abbottabad, Khyber Pakhtunkhwa, Pakistan

[2]Department of RF & Microwave, National Electronic Complex of Pakistan, Islamabad, Pakistan

Corresponding author: Irfanullah (e-mail: eengr@cuiatd.edu.pk).

ABSTRACT The probability of antenna array failure or malfunctioning cannot be ruled out, and hardware replacement of faulty elements is not always a viable solution. Therefore, academic and industrial interest in self-healing phased arrays are on the rise. In this work, the phase-only genetic algorithm (GA) optimization flow for the radiation pattern correction of a 4 × 4 phase faulty planar antenna array is proposed. Initially, a reference array pattern at the desired scan angle is generated. Then random phase faults are introduced across the 1 × 4 antenna elements in any one of 4 sub-arrays to produce maximum distortion in the reference radiation pattern of 4 × 4 planar array. The proposed GA re-computes the new excitation weights for the remaining non-faulty 3 sub-arrays to correct the overall radiation pattern of 4 × 4 array. This is achieved by calculating the array output power for reference and GA computed weights. The GA corrected patterns fairly follow the desired array patterns in terms of peak gain and reducing sidelobe levels for the desired scan angle. The efficiency of the optimized radiation patterns was evaluated in full-wave HFSS model and measurements validation. In this way, maintenance cost can be reduced with recovery of acceptable level of radiation pattern using software instead of physically replacing faulty antenna elements in the array.

INDEX TERMS Antenna array failure correction, faulty antenna array, genetic algorithm, phased array.

I. INTRODUCTION

PHASED array antenna used in aerial platforms (satellite and radar applications) suffer from either complete failure or malfunctioning of attenuators, phase shifters and amplifiers [1]. These failures/malfunctioning of radio frequency (RF) components connected to antenna elements causes distortion of main beam, increasing sidelobe levels and decrease in peak gain. Replacing defective array elements is not always a viable solution, so optimizing array weights of the active/non-faulty antenna elements is required. Active research work is going on in the field of antenna array failure detection and correction [2]. Most of the recent research work is focused on considering complete element failure, where the failed elements are considered to be non-active in the array. Therefore, the main focus is to optimize the weights on remaining active elements in the array to recover the radiation pattern. In this regard, various calibration [3,4] and optimization algorithms [5–7] have been proposed for antenna array failure detection and correction. The biologically inspired algorithms [8] have shown promising results for radiation pattern synthesis in antenna arrays. In particular, evolutionary algorithms (such as particle swarm optimization and genetic algorithm) have been explored for locating defective elements in the array [9,10], and array failure correction [11,12]. The design and synthesis of phased arrays for sidelobe level control without element failure using GA are reported in [13–16]. The use of GA for adaptive and smart arrays are discussed with details in [17,18].

In this work, genetic algorithm (GA) is investigated for recovering the main beam pattern in case of faulty sub-array elements in a planar phased array. That is, the antenna elements are not assumed to be completely failed, but phase malfunctioning of antenna elements is corrected with the GA optimization flow. Although any optimization algorithm can be used to address the antenna array failure correction, however, the choice of GA for the solution of proposed problem has proved very successful in applications in the field of electromagnetics [1, 22]. In the literature review summarized above, antenna array complete element failure is considered [1,2,11,12] except in a few papers [6,7], where partial element failure is investigated using analytical or numerical optimization techniques. However, in their findings, small phase error or perturbation correction is devised, mainly for calibrating the phased arrays, such as the work reported in [19]. The work in [28] and more recently in [29] are state of the art mechanisms for identifying fault locations in the beamforming arrays. The work in [30] is interesting and is related to our work as follows: In [30], the beamforming array is disturbed by the scatterer in its

vicinity, distorting its original pattern. Then cloaking is applied on the obstacle make it invisible to the beamforming array to get the optimal beamforming pattern. In many implementations, the attenuator and phase shifter in transmit-receive module can independently get defected. In our work we look at the scenario in which phase shifter get defected at sub-array level with uniform amplitudes. This would result in non-convex constraints for the optimization problem and genetic algorithm is therefore employed to solve the problem. The algorithm has been tested with random phase errors at sub-array level and works fine. In our proposed work, random phase fault at sub-array level in a planar array is considered for correcting the overall array pattern. This technique is highly beneficial for self-healing phased array systems, where faulty phase shifters cannot be replaced.

In recent years, a new direction in electromagnetism has been intensively developing, associated with the development of design technologies for devices for electrical or magnetic cloaking of material bodies [33]. In this work, GA is proposed to correct the radiation pattern of a faulty antenna array in the presence of random phase errors. This approach can also be extended as follows to correct the faulty patterns (uncloaked) from a near-field scattering by using the GA based cloaking. The proposed GA can be optimized for the array of cloaking cylinders/spherical shells to estimate their variable lengths, diameters and separation distances.

Remainder of the paper is organized as follows. Section II presents the pattern correction methodology, section III describes the full-wave simulation results, section IV discusses the measurements validation and section V finally concludes the paper.

II. PATTERN CORRECTION METHDOLOGY

The flow chart of radiation pattern correction scheme is shown in Fig. 1. It is divided into two parts: planar array modeling and genetic algorithm (GA) optimization flow. The planar array consists of 4 × 4 antenna elements modelled in a HFSS full-wave model. Initially, the reference array pattern $\boldsymbol{AP_{ref}}$ is generated at the desired scan angle using the standard antenna array theory. Then random phase faults at sub-array level are introduced, and the corresponding faulty array pattern is denoted as $\boldsymbol{AP_F}$. Finally, the GA optimization is invoked to estimate the corrected phase set, which is then applied on the planar array, and the corrected array pattern is denoted as $\boldsymbol{AP_C}$. The pattern correction mechanism was validated with measurements setup.

A. REFERENCE ARRAY PATTERN GENERATION

Consider a N × N planar array in xy plane with the z-axis pointing away from the broadside as shown in Fig. 2. There are N sub-arrays parallel to y-axis and are lying along x-axis. The inter-element spacing along both x and y directions is dx=dy=λ/2=1.5 cm at f=10 GHz. The expression for the reference array pattern (AP_{ref}) can be written as

$$AP_{ref} = e\,(\theta,\phi)\ \times AF \tag{1}$$

where e (θ,ϕ) is an individual element pattern, and the array factor (AF) is a function of amplitude weights, phase weights, individual antenna element position and frequency.

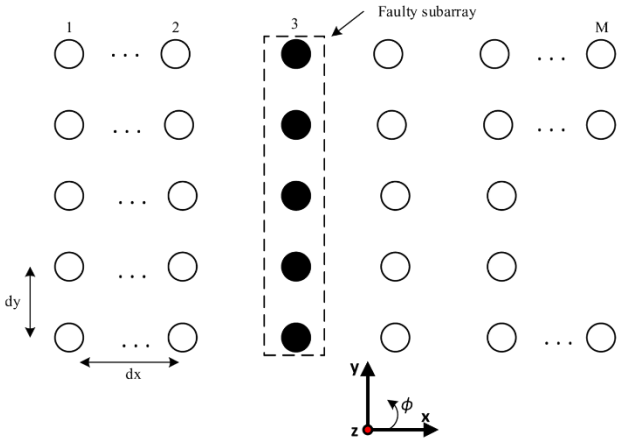

FIGURE 2. A faulty sub-array (shaded) in N × N planar array.

The expression for AF of a planar array in xy plane is given by [20]

$$AF = \sum_{n=1}^{N} W_n e^{j\psi_n}, \tag{2}$$

where

$$\psi_n = k(x_n u + y_n v), \tag{3}$$

and

$$u = \sin(\theta)\cos(\phi),\ v = \sin(\theta)\sin(\phi). \tag{4}$$

The (x_n, y_n) in (3) is the location of element n, θ is the elevation angle from z-axis, and ϕ is the azimuth angle measured from x-axis. The $W_n = a_n e^{j\delta_n}$ is the complex weight at element, $k = \frac{2\pi}{\lambda}$. For uniformly excited array, $a_n = 1$ on each element. The reference phase shift required at element n to generate the array pattern to steer the main beam at (θ_s, ϕ_s) is given by [20]

$$\delta_n = -k(x_n u + y_n v) \tag{5}$$

Equation (1) is used to generate the reference array pattern (AP_{ref}) with the phase set calculated in (5).

B. FAULTY ARRAY PATTERN GENERATION

The faulty array weights W_F are used in (2) to simulate the faulty beam patterns. In this work, random faulty array phase set δ_f ϵ[-π, π] are used in (2) instead of reference (original) phases calculated analytically in (5). For example, as shown in Fig. 2, the weights of faulty sub-array 2 are shaded, while the weights of non-faulty sub-arrays are not shaded. The array pattern due to faulty sub-array is generated using the following expression

$$AP_F = e\,(\theta,\phi)\ \times \sum_{n=1}^{N} e^{j\delta_f} e^{j\delta_n} e^{j\psi_n} \tag{6}$$

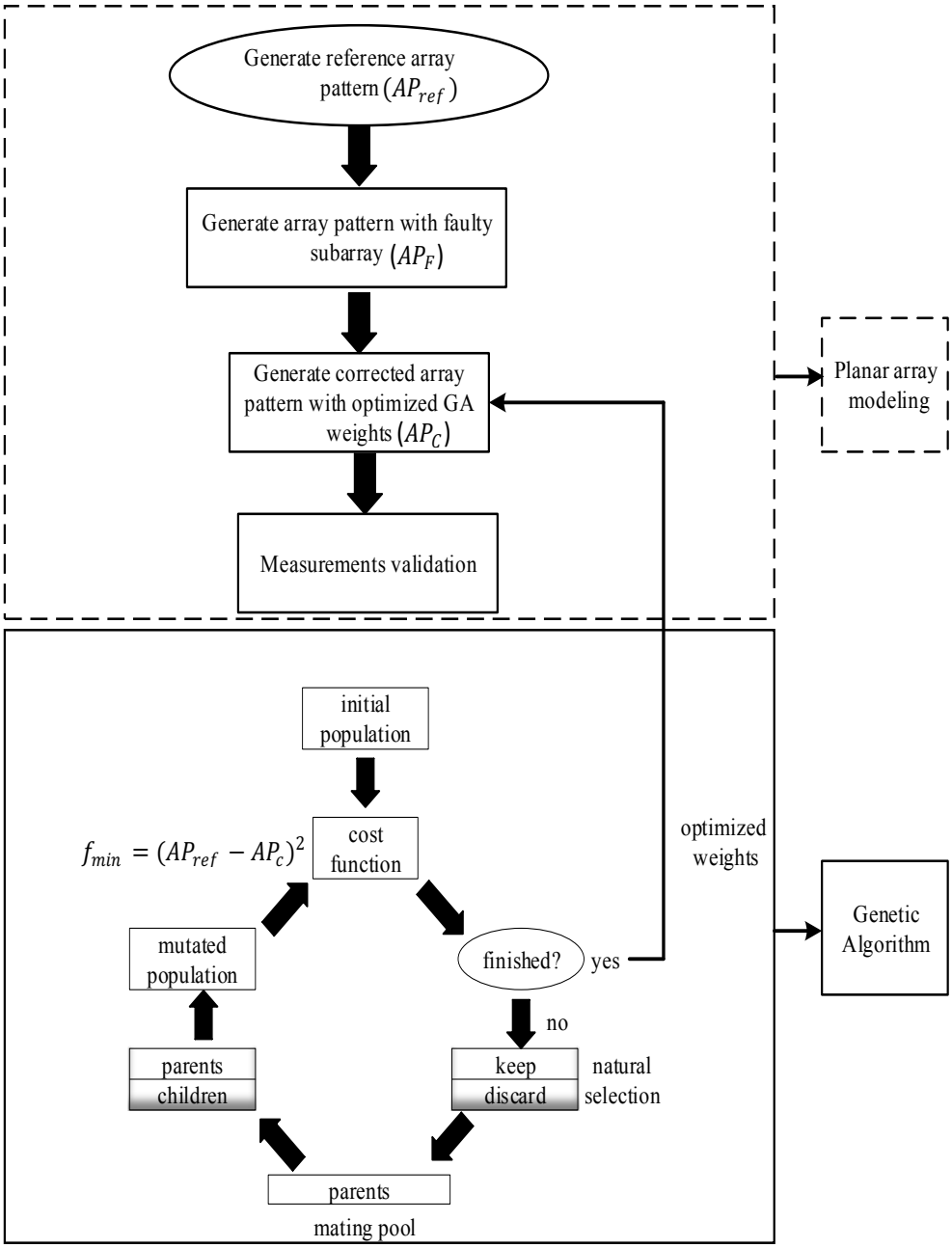

FIGURE 1. Radiation pattern correction mechanism.

C. PATTERN CORRECTION WITH GENETIC ALGORITHM (GA)

The genetic algorithm (GA) has been widely used in electromagnetics for various applications [21,22]. In the field of antenna arrays, GA has been mainly used for antenna array failure correction to recover the sidelobe levels due to edge elements failure across the array aperture [1]. To the best of our knowledge, no work is reported in the literature to investigate GA for the correction of radiation pattern due to faulty sub-arrays. The proposed work here investigates the GA for the correction of radiation pattern due to random phase faults at sub-arrays level across the array aperture. Therefore, unlike in [1], the proposed work does not consider element wise complete failure, but investigates correcting the pattern due to phase malfunctioning of sub-array using the GA. That is, in case of complete failure, the entire channel (attenuator, phase shifter, amplifier, and antenna) becomes inactive, while in the case of phase faulty sub-array, the channel antennas are working but with random uncorrected phases. Therefore, the problem formulation is to estimate the corrected phase set δ_c with GA to be applied on non-faulty sub-arrays for radiation pattern correction. The corrected array pattern (AP_C) due to optimized GA weights can be written as

$$AP_C = \mathrm{e}\,(\theta, \phi) \times \sum_{n=1}^{N} e^{j\delta_c} e^{j\psi_n} \quad (7)$$

where δ_c is the corrected phase set to be estimated with GA.

The flow chart to estimate the optimized array weights using GA for correcting the radiation pattern due to faulty sub-array is shown in Fig. 1. The GA starts with a list (population) of random solution set called chromosomes (i.e., phase set in this work). To evaluate each chromosome, a cost surface with objective function f_{min} is defined. This is the square of difference in array patterns (power level) between reference and corrected patterns subject to the given phase set. That is the objective function is given by

$$f_{min} = \left(AP_{ref} - AP_C\right)^2 \; \forall\, \theta \in [0, \pi], \phi \in [0, 2\pi] \quad (8)$$

Next, in the selection process, each chromosome is evaluated using (8). At this stage, chromosomes with low costs are selected for a mating pool. Two chromosomes for mating are randomly chosen using random number generator (such as roulette wheel). The selected parents are combined using genetic operator (crossover) to produce new offspring. The discarded chromosomes are replaced by new offspring in the population. Finally, some chromosomes in the new population may be mutated (random changes made to the chromosome), to introduce diversity into the new population and to create larger search space. The fitness of this generation is evaluated using (8), then a new generation begins with natural selection. This process continues until the optimum solution for computing corrected phase vector is obtained.

In this work, 360 samples of the radiation pattern were taken, which was initiated with a random population size of 1000, with 80% crossover rate, mutation rate of 12%, and elite chromosomes of 8%. The maximum number of generations set was 3000 for better convergence. The amplitudes were set to 1 and phase set $\rightarrow$ [0, 2π]. Minimization of the objective function in (8) will return optimized phase set of the non-faulty sub-arrays that can generate corrected array pattern in the presence of faulty sub-array. As can be seen in Fig. 3, the GA fairly converges after 200 generations with minimum error. The implementation steps for GA in MATLAB are given in Appendix B.

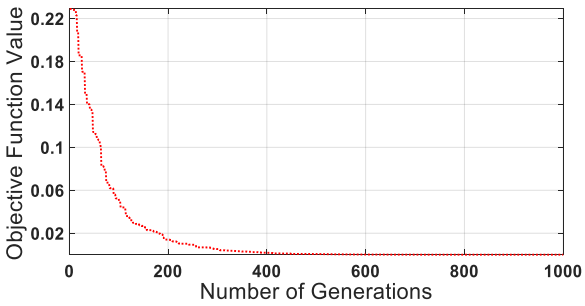

FIGURE 3. Convergence plot of the GA for a 4 × 4 planar array.

The statistical behavior of genetic algorithm for the phase error considering the broadside radiation pattern correction for phase faulty array is shown in Fig. 4. The plot presents the mean phase error for the respective sub-array along with a standard deviation of ±5° over 50 iterations. This tells that the algorithm is stable and effective in generating the desired radiation pattern in the presence of a phase faulty sub-array. Ideally for a broadside radiation pattern, the mean value should be around zero, but since the phase of second sub-array is made faulty randomly, the algorithm will optimize the phases of the remaining sub-arrays to successfully reconstruct the desired radiation pattern in a 4×4 planar array structure. The obtained mean error values and variance for each sub-array are given in Appendix A.

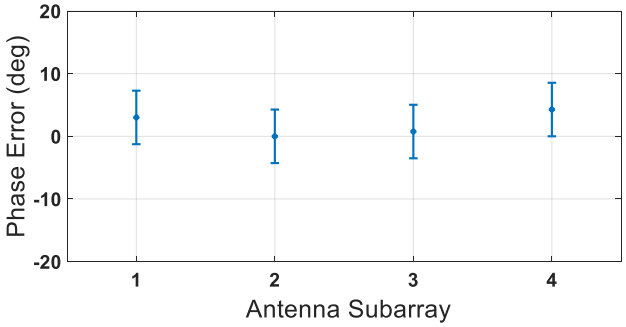

FIGURE 4. Mean and standard deviation plot for genetic algorithm in phase malfunctioning for the 4 × 4 planar array structure after 50 runs.

III. SIMULATION RESULTS

The pattern correction methodology with GA shown in Fig. 1 is evaluated in the subsequent sections.

A. PLANAR ARRAY MODELING RESULTS

A 4 × 4 planar microstrip array with inter-element spacing of $\frac{\lambda}{2}$ at f=10 GHz is simulated in HFSS simulator. Initially, the broadside ($\theta_s = 0^\circ, \phi_s = 0^\circ$) reference array pattern without any faulty sub-array is generated in HFSS using the analytical phase set from (5) and the simulated reference array pattern is shown in Fig. 5. Next, the array pattern with faulty sub-array is generated using (6) with three GA selected random phase faults. In this work, sub-array 2 in Fig. 2 is considered as faulty sub-array. Any random phase can be added to the elements in sub-array 2 to simulate it as a faulty sub-array as shown in the uncorrected patterns of Fig. 5 for three GA selected arbitrary phase faults. It is shown in Fig. 5(c) that by adding 180° phase fault in the sub-array elements generates maximum uncorrected radiation pattern by reducing the peak gain to 5 dB and increasing the sidelobe level to 8.5 dB as compared to the reference array pattern.

B. GENETIC ALGORITHM (GA) RESULTS

Next, the GA optimization flow is used to estimate the phase vector to recover the corrected radiation pattern. New GA optimized weights are applied on the non-faulty sub-arrays to calculate the corrected array pattern using (7). To accomplish this, the objective function in (8) is evaluated to minimize the error between reference and corrected array patterns. The iteration process of estimating correct phase vector continues until the objective function is satisfied. The

corrected broadside array patterns for the three phase faults are also shown on the same plot in Fig. 5. As can be seen, the corrected patterns with GA weights are exactly following the reference patterns. There is a maximum recovery of 5 dB peak gain in the corrected pattern over the uncorrected pattern as shown in Fig. 5(c). The maximum sidelobe level (SLL) is corrected by 8.5 dB with GA corrected pattern. The corrected mean phase vector estimated with GA after 50 runs is given in Appendix A. For comparison, the weight vectors for reference and uncorrected patterns are also given in Appendix A. The directivity of antenna array can be increased by reducing the sidelobe level using numerical/optimization techniques [31]. In our work, we have focused on correcting the faulty pattern using phase-only GA optimizer. The natural extension will be to use amplitude-phase GA to control the sidelobe level and increasing the gain simultaneously. In this way, signal-to-interference (SIR) can be improved as demonstrated in [32].

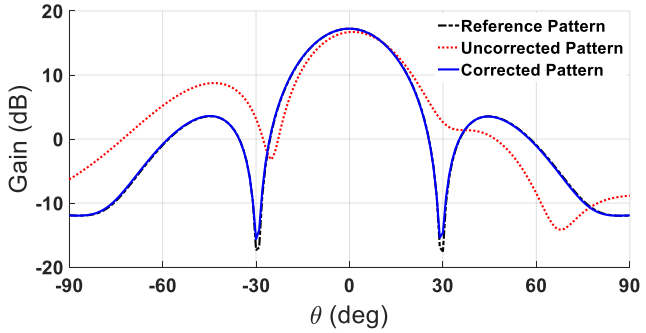

(a) phase fault of 45°

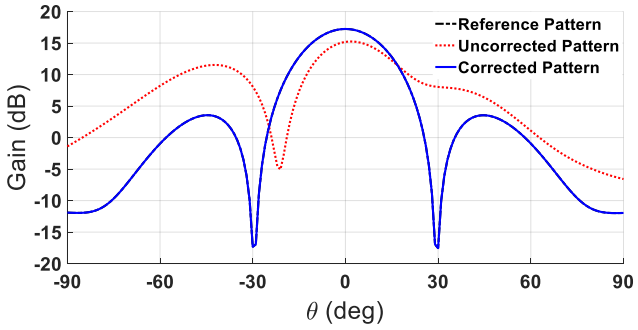

(b) phase fault of $\mathbf{90}^{\circ}$

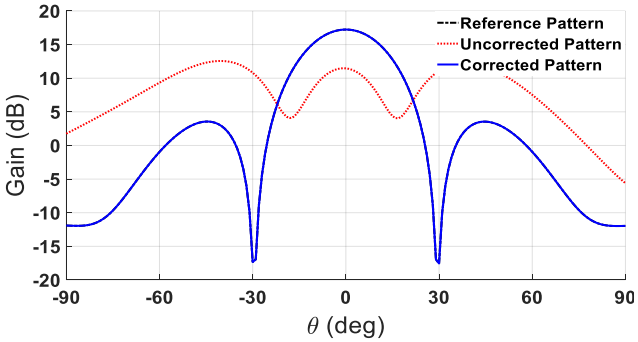

(c) phase fault of $\mathbf{180}^{\circ}$

FIGURE 5. Full-wave (HFSS) simulated radiation pattern correction with GA weights at broadside ($\theta_s = 0^{\circ}, \phi_s = 0^{\circ}$) for a 4 × 4 planar array with GA selected random phase faults at sub-array 2 (see Fig. 2).

Next, reference radiation patterns for 4 × 4 planar array without phase faults for scan angles of ($\phi_s = 0^{\circ}, \theta_s = 10^{\circ}, 20^{\circ}, 30^{\circ}, 40^{\circ}$) are generated using (5) in HFSS and are shown in Figs. 6-9. To generate maximum uncorrected patterns, the GA selected 180° phase is added to the element phases in the sub-array 2, and the resulting HFSS plots are shown in the same Figs. 6-9. As can be seen, for all scan cases, the reference patterns are distorted in terms of gain reduction and increasing SLLs. To evaluate the performance of GA, new phase weights are estimated over 50 runs for all the scan cases using the optimization flow discussed in section II. The corrected radiation patterns for all the scan cases using the optimized GA weights are also shown in Figs. 6-9. As can be seen, the corrected radiation patterns closely match the reference array patterns in terms of peak gain and SLL recovery. This validates that the phase-only GA can be used to recover array radiation patterns for any sub-array phase faults. The reference, uncorrected and GA corrected phases for scan angles are given in Appendix A.

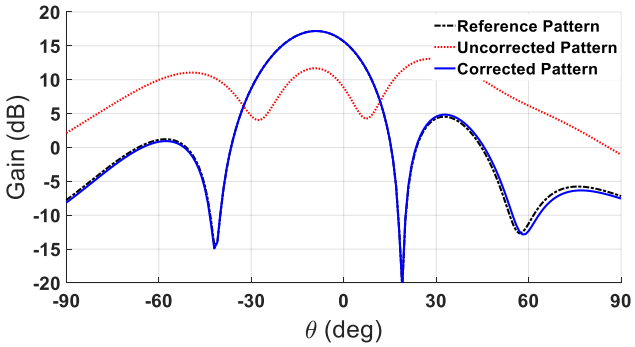

FIGURE. 6. Full-wave (HFSS) Simulated radiation pattern correction with GA weights at scan angle ($\theta_s = -10^{\circ}, \phi_s = 0^{\circ}$) for a 4 × 4 planar array with a GA selected phase fault of 180°.

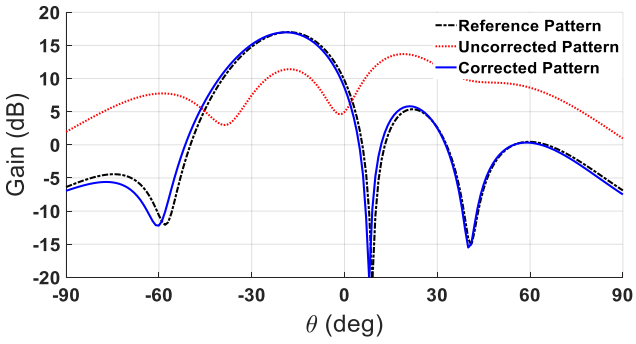

FIGURE. 7. Full-wave (HFSS) Simulated radiation pattern correction with GA weights at scan angle ($\theta_s = -20^{\circ}, \phi_s = 0^{\circ}$) for a 4 × 4 planar array with a GA selected phase fault of 180°.

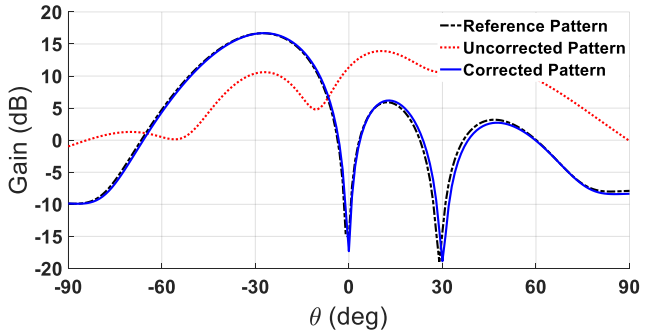

FIGURE. 8. Full-wave (HFSS) Simulated radiation pattern correction with GA weights at scan angle ($\theta_s = -30^\circ, \phi_s = 0^\circ$) for a 4 × 4 planar array with a GA selected phase fault of 180°.

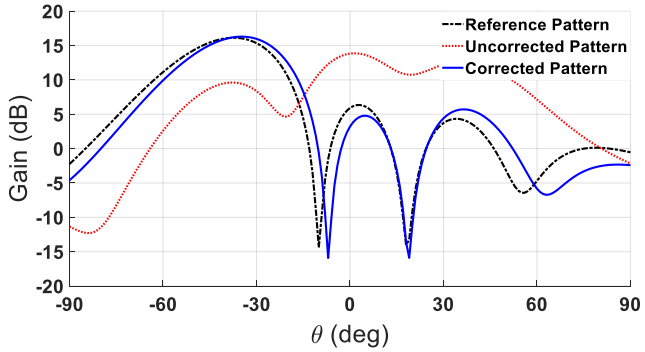

FIGURE. 9. Full-wave (HFSS) Simulated radiation pattern correction with GA weights at scan angle ($\theta_s = -40^\circ, \phi_s = 0^\circ$) for a 4 × 4 planar array with a GA selected phase fault of 180°.

IV. MEASUREMENTS VALIDATION

To validate the performance of GA, a 4 × 4 X-band Vivaldi antenna array reported in [23] is considered and is shown in Fig. 10(a). The 4 × 4 antenna array is divided into 4 sub-arrays of 1 × 4 antenna elements using the X-band power splitters. These 4 sub-arrays are excited with Analog Devices, Inc (ADI™) X-band phaser (ADAR1000-EVALZ) [24] to control the phases of antenna elements in each sub-array. The phases applied to each sub-array are controlled through ADI™ GUI. The complete measurements setup along with the planar array in the in-house anechoic chamber [25] is shown in Fig. 10. The measured reference, uncorrected and corrected array patterns for broadside and four scanning cases at f=10 GHz in xz-plane are shown in Figs. 11-15. Diamond Engineering™ desktop measurement software [26] was used to process the raw measurements data for gain patterns processing. The complete video of measurement setup in the calibrated measurement chamber is provided in [27].

The measured results in Figs. 11-15 shows similar trends as were discussed in simulated patterns (section III). The corrected gain patterns are fairly following the reference patterns in terms of peak gain and sidelobe levels. The cases of reference/corrected 30 and 40 degree scan in Fig. 14 are 4-5 degree off with reduced gain, while in simulation, they were 3 degree off (Figs. 8,9). For measurements purpose, the phases in Appendix A for reference, uncorrected and corrected gain patterns were implemented. This validates the accuracy of weights estimated with GA for the correction of radiation patterns. The deviations in measured results are due to the limitations of generating exact phases from the ADI™ phaser board with minimum of 2.8° phase error. In addition, for measurements purpose, the four sub-array channels were assumed to be exactly identical. However, in practice, there are always inherent amplitude/phase errors among the channels, which were not calibrated individually.

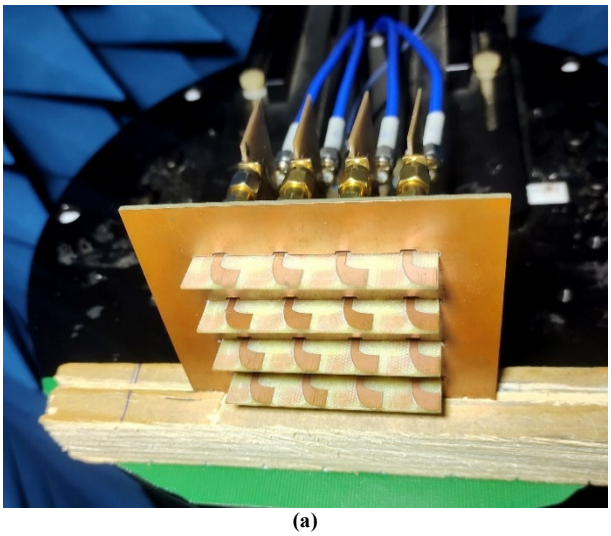

(a)

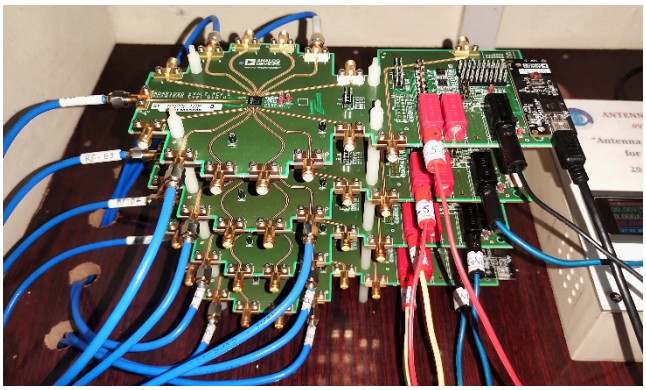

(b)

FIGURE. 10. Photographs of **(a)** X-band 4 × 4 Vivaldi antenna array [23] prototype in the anechoic chamber, **(b)** ADI™ X-band phaser [24].

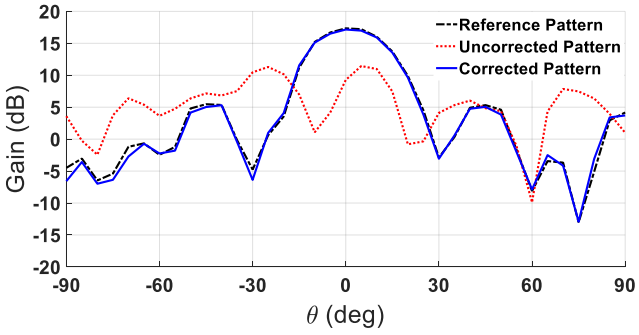

FIGURE. 11. Measured radiation pattern correction at f =10 GHz with GA weights at broadside ($\theta_s = 0^\circ, \phi_s = 0^\circ$) for a 4 × 4 planar array with GA selected phase fault of 180°.

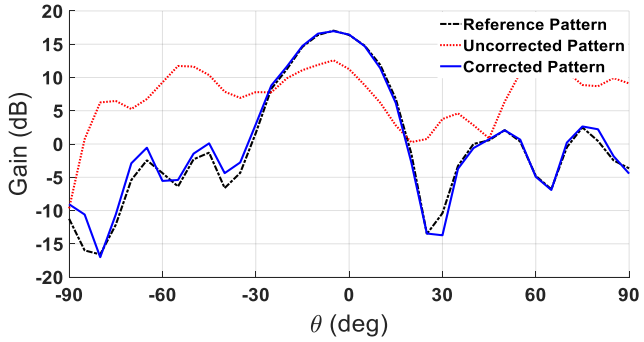

FIGURE. 12. Measured radiation pattern correction at f =10 GHz with GA weights at broadside ($\theta_s = -10^{\circ}, \phi_s = 0^{\circ}$) for a 4 × 4 planar array with GA selected phase fault of 180°.

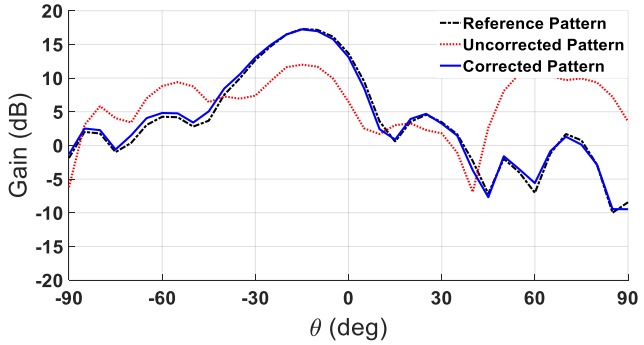

FIGURE. 13. Measured radiation pattern correction at f =10 GHz with GA weights at broadside ($\theta_s = -20^{\circ}, \phi_s = 0^{\circ}$) for a 4 × 4 planar array with GA selected phase fault of 180°.

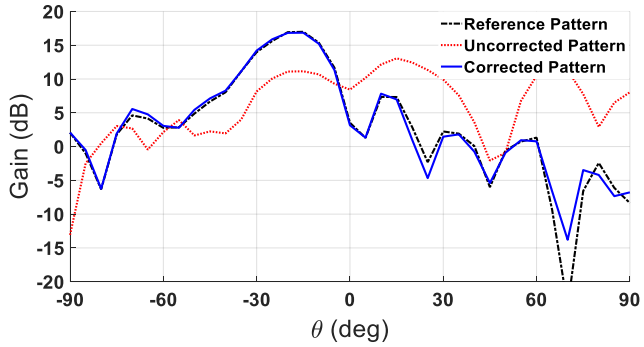

FIGURE. 14. Measured radiation pattern correction at f =10 GHz with GA weights at broadside ($\theta_s = -30^{\circ}, \phi_s = 0^{\circ}$) for a 4 × 4 planar array with GA selected phase fault of 180°.

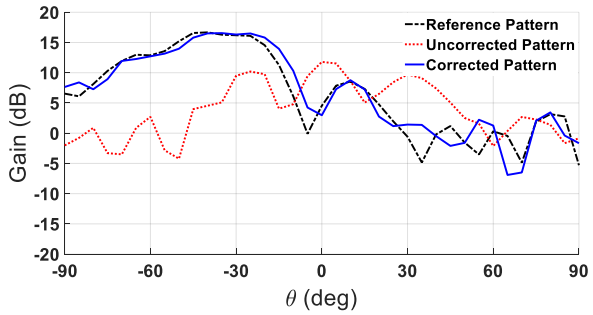

FIGURE. 15. Measured radiation pattern correction at f =10 GHz with GA weights at broadside ($\theta_s = -40^{\circ}, \phi_s = 0^{\circ}$) for a 4 × 4 planar array with GA selected phase fault of 180°.

V. CONCLUSION

The radiation pattern recovery of a faulty 4 × 4 X-band planar antenna array with genetic algorithm (GA) optimized weights is investigated. The phase correction mechanism using GA optimization flow with phase-only fault at sub-array level is proposed. It is shown that the proposed optimization algorithm can recover the desired radiation pattern in case of any phase faulty sub-array. The measurements validation indicate that the proposed GA can compute the optimized array weights for non-faulty sub-arrays to recover the peak gain and first sidelobe level of radiation patterns close to the reference array patterns. This work can be extended to malfunctioning amplitude weights for sidelobe level and nulls control.

ACKNOWLEDGMENT

This work is funded by the HEC-NRPU, Pakistan via Project No. 20-14696/NRPU/R&D/HEC/2021.

REFERENCES

[1] O. P. Acharya, and A. Patnaik, "Antenna array failure correction," *IEEE Antennas Propag. Mag.*, vol. 59, no. 6, pp. 106–115, Dec. 2017. DOI: 10.1109/MAP.2017.2752683.

[2] Y-S Chen, and I-L Tsai, "Detection and correction of element failures using a cumulative sum scheme for active phased arrays," *IEEE Access*, vol. 6, pp. 8797–8809, Feb. 2018. DOI: 10.1109/ACCESS.2018.2803791.

[3] S. Kim, H-J. Dong, J-W. Yu, and H. L. Lee, "Phased array calibration system with high accuracy and low complexity," *Alex. Eng. J.*, vol. 69, pp. 759–770, April 2023. DOI: 10.1016/j.aej.2023.02.026.

[4] J. A. Rodriguez-Gonzalez *et al.,* "Rapid method for finding faulty elements in antenna arrays using far field pattern samples," in *3rd EuCAP,* Berlin, Germany, 2009, pp. 1–5, DOI: 10.1109/TAP.2009.2019915.

[5] S. C. Liu, "A fault correction technique for phased array antennas," in *IEEE AP-S International Symposium (Digest)*, Chicago, IL, USA, 1992, pp. 1–4, DOI: 10.1109/APS.1992.221727.

[6] S. U. Khan *et al.*, "Correction of faulty sensors in phased array radars using symmetrical sensor failure technique and cultural algorithm with differential evolution," *The Sci. World J.*, vol. 2014, pp. 1–10, Jan. 2014. DOI: 10.1155/2014/852539.

[7] Y. Yang *et al.*, "A novel channel amplitude and phase correction algorithm based on phased array space-based TT&C communication," in *4th International CMAEE*, Beijing, China, 2020, pp. 1–6, DOI: 10.1088/1742-6596/1626/1/012026.

[8] P. Rocca and R. L. Haupt, "Biologically inspired optimization of antenna arrays," *The ACES Journal*, vol. 29, no. 12, pp. 1047–1059, 2014.

[9] O. P. Acharya, A. Patnaik and B. Choudhury, "A PSO application for locating defective elements in antenna arrays," in *World Congress on NaBIC*, Coimbatore, India, 2009, pp. 1094–1098, DOI: 10.1109/NABIC.2009.5393809.

[10] J. A. Rodriguez-Gonzalez *et al.,* "Finding defective elements in planar arrays using genetic algorithms," *PIERS*, vol. 29, pp. 25–37, 2000. DOI: 10.2528/PIER00011401.

[11] B-K Yeo and Y. Lu, "Array failure correction with a genetic algorithm," *IEEE Trans. Antennas Propag.*, vol. 47, no. 5, pp. 823–828, May 1999. DOI: 10.1109/8.774136.

[12] N. Boopalan, A. K. Ramasamy, F. Nagi, and A. A. Alkahtani, "Planar array failed element(s) radiation pattern correction: a

comparison," *Appl. Sci*, vol. 11, pp. 1–19, Oct. 2021. DOI: 10.3390/app11199234.

[13] F. J. Ares-Pena, J. A. Rodriguez-Gonzalez, E. Villanueva-Lopez, S. R. Rengarajan, "Genetic algorithms in the design and optimization of antenna array patterns," *IEEE Trans. Antennas Propag.*, vol. 47, no. 3, pp. 506–510, Mar. 1999 DOI: 10.1109/8.768786.

[14] D. Marcano and F. Duran, "Synthesis of antenna arrays using genetic algorithms," *IEEE Antennas Propag. Mag.*, vol. 42, no. 3, pp. 12–20, June 2000. DOI: 10.1109/74.848944.

[15] Y. Wang, S. Gao, H. Yu, and Z. Tang, "Synthesis of antenna array by complex-valued genetic algorithm," *IJCSNS*, vol. 11, no. 1, pp. 91–96,Jan.2011.URL: http://paper.ijcsns.org/07_book/201101/20110113.pdf

[16] Y. Fan, Y., R. In, and B. Liu, "Synthesis of antenna arrays using a modified complex number coded genetic algorithm," in *IEEE AP-S Symposium*. Monterey, CA, USA, 2004, pp. 1–4. DOI: 10.1109/APS.2004.1331923.

[17] R. L. Haupt, "Adaptive antenna arrays using a genetic algorithm," *IEEE Mountain Workshop on Adaptive and Learning Systems*, The Logan, UT, USA, 2006, pp. 1–6, DOI: 10.1109/SMCALS.2006.250724.

[18] R. L. Haupt, "Genetic algorithm applications for phased arrays," *The ACES Journal*, vol. 21, no. 3, pp. 325–336, Nov. 2006.

[19] S. H. Son, S. Y. Eom, S. I. Jeon, and W. Hwang, "Automatic phase correction of phased array antennas by a genetic algorithm," *IEEE Trans. Antennas Propag.*, vol. 56, no. 8, pp. 2751–2754, Aug. 2008. DOI: 10.1109/TAP.2008.927575.

[20] R. L. Haupt, *Antenna Arrays: A Computational Approach*. Wiley-IEEE Press, 2010, pp. 552. ISBN: 978-0-470-93743-3.

[21] R. L. Haupt, and S. E. Haupt, *Practical Genetic Algorithms. 2nd ed.* Wiley-Interscience, 2004, pp. 288. ISBN: 978-0-471-45565-3.

[22] R. L. Haupt, and D. H. Werner, Genetic *Algorithms in Electromagnetics*. Wiley-IEEE Press, 2007, pp. 320. ISBN: 978-0-471-48889-7.

[23] J. Tahir and A. I. Najam, "Design of 4×4 antenna array for actively electronic scanned array (AESA) radars," in *15th IBCAST*, Islamabad, Pakistan, 2018, pp. 853–857, DOI: 10.1109/IBCAST.2018.8312325.

[24] Analog Devices, Inc (ADI™). *EVAL-ADAR1000 (Evaluation Board))*. [Online] Cited 2024-04-29. Available at: https://www.analog.com/media/en/technical-documentation/user-guides/ADAR1000-EVALZ-UG-1283.pdf

[25] COMSATS University Islamabad Abbottabad Campus. *Anechoic Chamber*. [Online] Cited 2024-04-29. Available at: https://www.cuiatd.edu.pk/electrical-computer-engineering/research-project-cba/signal-absorber-installation/

[26] Diamond Engineering. *Antenna measurement system*. [Online] Cited 2024-04-29. Available at: http://www.diamondeng.net/PDF/DAMS_5000.pdf

[27] Youtube. [Online] Cited 2024-04-29. Available at: https://youtu.be/3eEuH0tYq2s

[28] P. Smith, C. Furse, and J. Gunther, "Analysis of spread spectrum time domain reflectometry for wire fault location," *IEEE Sensors*, vol. 5, no. 6, pp. 1469–1478, Nov. 2005. DOI: 10.1109/JSEN.2005.858964.

[29] S. Zhu, C. Han, Y. Meng, J. Xu, and T. An, "Embryonics based phased array antenna structure with self-repair ability," *IEEE Access*, vol. 8, pp. 209660–209673, Nov. 2020. DOI: 10.1109/ACCESS.2020.3038857.

[30] C. Valagiannopoulos, and V. Kovanis, "Engineering the emission of laser arrays to nullify the jamming from passive obstacles," *Photonics Research*, vol. 6, no. 8, pp. A43-A50, 2018. DOI: https://doi.org/10.1364/PRJ.6.000A43.

[31] Y-X. Zhang, Y-C. Jiao, and L. Zhang, "Antenna array directivity maximization with sidelobe level constraints using convex optimization," *IEEE Trans. Antennas Propag.*, vol. 69, no. 4, pp. 2041–2052, Apr. 2021. DOI: 10.1109/TAP.2020.3026886.

[32] C. Valagiannopoulos, T. A. Tsiftsis, and V. Kovanis, "Metasurface-enabled interference mitigation in visible light communication architectures," *Journal of Optics*, vol. 21, no. 11, pp. 1–11, Oct. 2019. DOI: 10.1088/2040-8986/ab4c08.

[33] P. Alitalo, C. Valagiannopoulos, and S. A. Tretyakov, "Simple cloak for antenna blockage reduction," *2011 IEEE International Symposium on Antennas and Propagation (APSURSI),* Spokane, WA, USA, 2011, pp. 669–672. DOI: 10.1109/APS.2011.5996800.

APPENDIX A: The Array Weights (The Values Highlighted in Red Represents the Phases on Faulty Subarray)

Subarray No.	Case 1: Broadside Correction								
	Original	Uncorrected	Corrected	Uncorrected	Corrected	Uncorrected	Corrected		
	Phase (°)	Phases (°)	Mean Phases (°)	Phases (°)	Mean Phases (°)	Phases (°)	Mean Phases (°) 50 iteration	Mean Error (°)	Standard Deviation (°)
1	0	0	43.40	0	87.72	0	175.51	-4.50	3.02
2	0	0 + 45	45.00	0 + 90	90.00	0 + 180	180.00	0	0.00
3	0	0	44.26	0	88.78	0	179.93	-0.06	0.76
4	0	0	42.89	0	88.05	0	174.47	-5.54	4.27

Subarray No.	Case 2: Scan –10˚ Correction			Case 3: Scan –20˚ Correction		
	Original	Uncorrected	Corrected	Original	Uncorrected	Corrected
	Phase (°)	Phases (°)	Phases (°)	Phase (°)	Phases (°)	Phases (°)
1	0	0	238.38	0	0	301.09
2	30	30 + 180	210.00	60	60 + 180	240.00
3	60	60	178.12	120	120	174.18
4	90	90	149.74	180	180	112.91

Subarray No.	Case 4: Scan –30˚ Correction			Case 5: Scan –40˚ Correction		
	Original	Uncorrected	Corrected	Original	Uncorrected	Corrected
	Phase (°)	Phases (°)	Phases (°)	Phase (°)	Phases (°)	Phases (°)
1	0	0	356.37	0	0	59.12
2	90	90 + 180	270.00	120	120+180	300.00
3	180	180	179.09	240	240	198.55
4	270	270	91.23	360	360	79.44

APPENDIX B: Implementation steps for GA in MATLAB

- Step 1: Generate a random population matrix of size $N_{pop} \times N$. Where $N_{pop} = 1000$ (population size) and N is the random phase set on the elements of subarrays.
- Step 2: Evaluate objective function using equation (8) for each row.
- Step 3: Discard high cost rows (natural selection).
- Step 4: Combine and change selected rows to make new rows (mating, crossover and mutation).
- Step 5: Evaluate objective function using (8) for new and altered rows.
- Step 6: Check convergence. If YES, then the estimated weights are optimized. If NO, then go to step 2.